

# Early-stage real-time dynamics of interlayer $sp^3$ -bond formation by visible-light irradiation of graphite

Keita Nishioka<sup>1</sup> and Keiichiro Nasu<sup>1,2</sup><sup>1</sup>*Solid State Theory Division, Institute of Materials Structure Science, High Energy Accelerator Research Organization (KEK), 1-1 Oho, Tsukuba, Ibaraki 305-0801, Japan*<sup>2</sup>*CREST JST, Graduate University for Advanced Study, 1-1 Oho, Tsukuba, Ibaraki 305-0801, Japan*

(Received 31 August 2009; published 14 December 2009)

We theoretically study the early-stage real-time dynamics of the interlayer  $\sigma$ -bond formation by visible-light irradiation of graphite crystal. An electron-hole pair, generated as an interlayer charge-transfer excitation in the visible region, mostly dissipates away into the two-dimensional semimetallic electronic continuum as plus and minus free carriers. However, by a small but finite probability, this electron-hole pair self-localizes during the lattice relaxation, resulting in a local interlayer contraction to form a  $\sigma$  bond. Our theory for this dynamics is composed of two parts. The first part describes the quantum and spontaneous breakage of the translational symmetry, or the self-localization of this electron-hole pair, in a simplified way. While the subsequent second one, by using a Brenner's potential, describes the classical dynamics of a further local lattice distortion which occurs after this self-localization and also describes the final interlayer  $\sigma$ -bond formation. We thus estimate this probability of self-localization and show the conditions that the interlayer  $\sigma$  bond can be formed. Consequently, we find that the self-localization occurs by the probability of about 2% and the subsequent bond formation is achieved when the excitation energy is more than 4.5 eV corresponding to about three visible photons.

DOI: [10.1103/PhysRevB.80.235420](https://doi.org/10.1103/PhysRevB.80.235420)

PACS number(s): 78.90.+t, 64.70.Nd, 78.20.Bh, 31.15.xv

## I. INTRODUCTION

Various problems related with the conversion from the  $sp^2$ -bonded graphite to the  $sp^3$ -bonded diamond have been very intensively studied, both experimentally<sup>1-4</sup> and theoretically.<sup>5-8</sup> The graphite is the most stable phase within various possible structures of carbon crystals, being 0.02 eV/atom lower than the diamond at absolute zero temperature and atmospheric pressure.<sup>9</sup> The energy barrier between them is estimated to be about 0.3–0.4 eV/atom by the local-density approximation (LDA).<sup>5,6</sup> In this LDA calculation, however, the whole carbons transform simultaneously and uniformly from the graphite to the diamond. Therefore, a large amount of energy is required for this conversion. From this fact, the conventional conversion is carried out globally and macroscopically under high temperature and high pressure (3000 °C, 15 GPa),<sup>1,2</sup> or under the irradiation of strong x ray.<sup>3,4</sup>

In contrast, recently, Kanasaki *et al.*<sup>10</sup> experimentally proposed a quite different conversion method from the above methods, which achieves the graphite-diamond transition stepwise by the irradiation of visible light.<sup>11</sup> In this transition, a long-lived locally stable macroscopic phase is generated by the visible photon excitations during lattice relaxation, and expected to finally result in the diamond phase. This nonequilibrium phase transition is known as a kind of photoinduced structural phase transition.<sup>12,13</sup> According to their experiment,<sup>10</sup> when the graphite layers are illuminated perpendicularly by femtosecond pulse laser with the energy 1.57 eV, a photoinduced nanoscale new domain, including more than 1000 carbons, appears in the graphite surface. The scanning tunneling microscopy revealed such a unique new domain structure that one third of carbons sinks down, and residual two thirds rise up from the layer in each six-

membered ring. The sinking down carbons are expected to form  $\sigma$  bonds between the graphite layers, leading to the  $sp^3$  structure of the diamond. The resultant domain is stable for several days at room temperature. We should note that the light polarized parallel to the layer gives no effect. This means only the interlayer charge-transfer excitation from one layer to its neighboring layer can trigger this phase transition. It should be also noted that the exciting light should be a femtosecond pulse, while a picosecond pulse gives almost no contribution. This means only a transient generation of an excited electronic wave packet can efficiently trigger this phase transition, while a monochromatic or stationary electronic excitation is not effective. Moreover, this photoinduced transition is a nonlinear multiphoton process, but less than the ten-photon one.

The nanoscale domain, thus generated locally and microscopically, is not the conventional diamond, but an intermediate state between the graphite and the diamond. This kind of the intermediate structure is called “diaphite.”<sup>10,14</sup> Further pulse excitation will generate a lot of such domains, and they combine with each other, proliferate and will finally result in the macroscopic diamond phase.

In our previous research, we have already calculated the adiabatic path from the starting graphite to the small diaphite domain, by means of the LDA (Ref. 15) and also by the semiempirical Brenner's theory.<sup>16</sup> These two results show that the diaphite domain can be nucleated by a few visible photon excitations and is stable against the thermal fluctuation at room temperature. The local density of electronic state due to this diaphite domain also has been calculated, and a pseudogap has been revealed to open, leading to the existence of the insulator domain immersed in the semimetallic graphite. Thus, the adiabatic property of the phase transition from the graphite to the diaphite domain has been already well clarified theoretically.

However, this type of nonequilibrium phase transition occurs dynamically. Hence, in this paper, we will theoretically investigate the dynamics of the nonequilibrium phase transition from the graphite to the diaphite domain. Our theory for this dynamics is composed of two parts. The first part describes the quantum and spontaneous breakage of the translational symmetry, or the self-localization of an electron-hole pair, in a simplified way. While the subsequent second one, by using a Brenner's potential, describes the classical dynamics of a further local lattice distortion after this self-localization and also describes the final interlayer  $\sigma$ -bond formation.

## II. OUR SCENARIO

Let us now explain the concept of the early-time process of the photoinduced phase transition from the graphite to the diaphite domain. The irradiation of visible light polarized perpendicular to the graphite layer causes the interlayer charge-transfer excitation, resulting in an electron-hole pair spanning neighboring two layers. The wavelength of visible light is quite larger than the lattice constant of the graphite. This means that the wave vector of the visible photon is almost zero, because it is extremely smaller than the wave vectors of an electron, a hole and phonons in the first Brillouin zone. After the irradiation of visible light, therefore, an electron-hole pair excitation can occur any place in the graphite layer. Thus, at the Franck-Condon state immediately after the photoexcitation, the excitations strongly interfere with each other quantum mechanically under the condition that the total number of the excitations is equal to one. Consequently, the initial excited state is the Bloch wave whose total wave vector is almost zero, having the full translational symmetry.

On the other hand, at the Franck-Condon state, the electron-hole pair is quite unstable, and easily dissipates into the two-dimensional (2D) semimetallic continuum electronic state as plus and minus free carriers, because of the good conductivity of the graphite. However, by a small but finite probability, the electron-hole pair is expected to become stable as the lattice relaxation proceeds, being bound with each other just like an exciton, through the interlayer Coulomb attraction. This excitonlike state will self-localize at a certain point of the layer, by contracting the interlayer distance only around it. After the large contraction of the interlayer distance, the quantum coherency between the self-localized exciton states is lost, even if the excitations are at the neighboring lattice sites. This relaxation with the lattice distortion from the Bloch wave to the self-localized state can occur spontaneously anywhere of the lattice at the same probability. It is only due to the quantum fluctuations, and can occur even at absolute zero temperature. As a result, the translational symmetry of the exciton state is broken. Thus, by locally contracting the interlayer distance, an interlayer  $\sigma$  bond is formed. It opens up a pseudoenergy gap at the Fermi level, and a tiny insulating domain appears in the semimetallic continuum. Through further pulse excitations by several visible photons, a lot of  $\sigma$  bonds are formed stepwise, and then the diaphite structure is expected to appear macroscopically in the graphite layer.

In order to qualitatively clarify the mechanism of this nonequilibrium phase transition, we use the following two-step theoretical methodology. First, we describe the self-localization of an electron-hole pair, or the spontaneous translational symmetry breaking full quantum mechanically. By solving the quantum time development of the whole system, we calculate the dynamics of an electron-hole pair, which is photoexcited at the Franck-Condon state and finally self-localizes. Once the quantum coherency between excitations is thus lost by contracting the interlayer distance, the subsequent  $\sigma$ -bond formation can be taken into account in a local, adiabatic and classical picture, including the excess energy dissipation as phonons.

Therefore, we have to partly approximate the dynamics of the bond formation as a classical process. In that case, we use a molecular dynamics (MD) with the Brenner's potential<sup>9</sup> ( $\equiv E_b$ ), which is given as

$$E_b = \sum_{i < j} \{V_R(r_{ij}) - \bar{B}_{ij}V_A(r_{ij})\}. \quad (1)$$

where  $V_R$  and  $V_A$  are repulsive and attractive radial two-body pair potentials as a function of the distance  $r_{ij}$  between  $i$ th and  $j$ th carbons. The bond order function  $\bar{B}_{ij}$  takes into account the three- or four-body force as a function of the bond angle, in contrast to the ordinary Lennard-John's two-body-type potential. In our calculation, we adopt the Brenner's potential I in the original method, which can reproduce almost all existing experimental and theoretical data of various carbon clusters. In fact, it can well reproduces the binding energy of the graphite and the diamond.<sup>9</sup>

## III. PROBABILITY OF SELF-LOCALIZATION

As mentioned before, the self-localization of an electron-hole pair in the graphite strongly competes against the quantum diffusion as free carriers. Thus, one of the most important points of the present photoinduced phase transition is to estimate how large the probability of self-localization is, relative to the free carrier type relaxation. For this reason, we calculate the early-time nonadiabatic dynamics of an electron-hole pair, which is almost instantaneously excited by a femtosecond photon pulse. In our calculation, we focus only in the vicinity of the Franck-Condon state, and determine the branching ratio between these two relaxation channels, that is, the free carrier type relaxation versus the self-localization.

### A. Model and method

Our process starts from the electron-hole pair excited by the visible photon, spanning neighboring two layers. Before this excitation, the graphite layers have a 2D semimetallic continuum electronic state, with only a weak interlayer interaction. Therefore, we consider a minimal model with only a pair of distant layers, consisting of an electron, a hole and local phonons whose mode contracts the interlayer distance. Throughout this paper, we set  $\hbar = 1$ . The model Hamiltonian ( $\equiv H$ ) is given as

$$H = H_{eh} + H_{ph} + H_c. \quad (2)$$

The first term denotes the transfer energy of an electron and a hole given as

$$H_{eh} = \sum_{i=1,2} \sum_{j=1,2} \sum_{\ell, \ell'} T(\ell - \ell') a_{\ell ij}^\dagger a_{\ell' ij}, \quad (3)$$

where  $a_{\ell ij}^\dagger$  is the creation operator of an electron ( $i=1$ ) or a hole ( $i=2$ ) at the  $\ell$ th site of the  $j(=1, 2)$ th layer. For simplicity, the spin is neglected.  $T(\ell)$  is the intersite transfer energy and given through the Fourier transformation of the dispersion relation [ $\equiv E(k)$ ],

$$T(\ell) = \frac{1}{N} \sum_k E(k) e^{-ik \cdot \ell}, \quad (4)$$

where  $N$  is the total number of the lattice sites in a layer.

Around the Fermi level of a graphite layer, there are several energy bands coming from the hybridization between  $2s$  and  $2p_\pi$  orbitals of carbon atoms. They are almost symmetric with respect to the Fermi level, and extend in a wide energy region from about  $-20$  to  $20$  eV. In the present paper, however, we are interested only in the visible excitations with the energy  $\sim 4$  eV around the Fermi level, and this region is mainly related with  $2p_\pi$  orbitals of carbons. Hence, we assume this energy dispersion  $E(k)$  to be V shape (the Dirac cone), given as

$$E(k) = \sqrt{k_x^2 + k_y^2}, \quad |k_x| \leq \pi, \quad |k_y| \leq \pi, \quad (5)$$

wherein  $k_x$  and  $k_y$  are the Cartesian components of the wave vector  $k$ , and the lattice structure of the layer is also assumed to be the 2D square lattice, for simplicity. The electronic state on which this Hamiltonian is mainly based, is the  $2p_\pi$  orbital of carbons. This situation is quite simple, but well describes the semimetallicity of the graphite layer around the Fermi level. The Fermi point of our model is at the  $\Gamma$  point of the Brillouin zone, while that of the real graphite is at the  $K$  point. However, this difference gives no serious effect for our final conclusion, since the Fermi point can be moved to other points by an appropriate gauge transformation.

The second term of Eq. (2) denotes a localized phonon at the  $\ell$ th site and given as

$$H_{ph} = \sum_\ell \left\{ \frac{\omega}{2} (P_\ell^2 + Q_\ell^2) + \sum_{n \geq 4} 'c_n Q_\ell^n \right\}, \quad (6)$$

$$[Q_\ell, P_\ell] = i. \quad (7)$$

Here  $P_\ell$  and  $Q_\ell$  are the dimensionless momentum and coordinate, respectively. This phonon mode corresponds to the intruded displacement of two opposite carbons perpendicular to the layers, as shown in Fig. 1(a). The two opposite carbons are assumed to be intruded at the same distance. We also take anharmonicity of the phonon into account and  $\Sigma'$  means the summation over  $n(\geq 4)$  only of the even order. As already mentioned before,  $H_{eh}$  in Eq. (3) is mainly based on the  $2p_\pi$  orbital of carbons in each layer. However, as  $Q_\ell$  increases, the interlayer hybridization between  $2p_\pi$  orbitals gradually occurs, as well as intralayer and interlayer hybridization between  $2s$  and  $2p_\pi$  orbitals. The anharmonicity in Eq. (6)

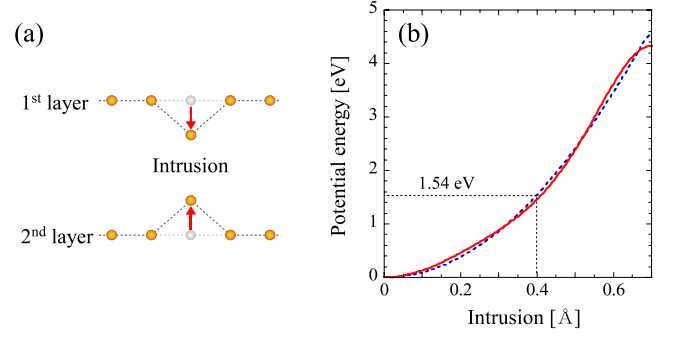


FIG. 1. (Color online) (a) A schematic representation of the displacement of two opposite carbons in the local phonon mode. (b) The potential energy calculated by using the Brenner's potential (dashed line) and the fitted curve by the tenth-order polynomial (solid line). The intrusion in the horizontal axis means the distance that the one carbon is intruded from the original position.

partly denotes this hybridization effect phenomenologically. The parameters  $\omega$  and  $c_n$  are determined so as to reproduce the potential energy when only two opposite carbons of distant graphite layers are intruded. We calculate the potential energy by using the Brenner's potential.<sup>9</sup> In Fig. 1(b), the result of the Brenner's potential and the fitted curve are shown by dashed and solid lines, respectively. The intrusion in the horizontal axis means the distance that the one carbon is intruded from the original position, hence, the intercarbon distance contracts twice. In order to reproduce this potential, we take the anharmonic terms up to the tenth order. The values of the parameters are as follows:

$$\begin{aligned} \omega &= 9.847 \times 10^{-2} \text{ eV}, \\ c_4 &= -9.280 \times 10^{-4} \text{ eV}, \\ c_6 &= 1.683 \times 10^{-5} \text{ eV}, \\ c_8 &= -1.134 \times 10^{-7} \text{ eV}, \\ c_{10} &= 2.417 \times 10^{-10} \text{ eV}. \end{aligned} \quad (8)$$

$H_c$  in Eq. (2) denotes the interlayer Coulomb interaction between the optically excited electron and the hole, and is given by

$$H_c = - \sum_\ell U(Q_\ell) (n_{\ell 11} n_{\ell 22} + n_{\ell 12} n_{\ell 21}), \quad (9)$$

where  $n_{\ell ij} = a_{\ell ij}^\dagger a_{\ell ij}$ .  $U(Q_\ell)$  is the phonon-dependent Coulomb interaction which is assumed to be linear, as

$$U(Q_\ell) = U_0 + U_d Q_\ell. \quad (10)$$

Here,  $U_0$  corresponds to the electron-hole coupling in the undistorted graphite and is taken to be 1.5 eV. The value of  $U_d$  is set to 0.225 eV. These values for  $U_0$  and  $U_d$  come from the Mataga-Nishimoto formula.<sup>11,17</sup>

According to the Cho-Toyozawa theory,<sup>18</sup> we define a basis set of our minimal model as a Bloch wave composed of electron-hole-phonon coupled states as,

$$|\Delta, m\rangle = \frac{1}{\sqrt{N}} \sum_{\ell} e^{-ik_p \cdot \ell} a_{\ell+\Delta, 11}^{\dagger} a_{\ell, 22}^{\dagger} \frac{(b_{\ell}^{\dagger})^m}{\sqrt{m!}} |0\rangle, \quad (11)$$

$$b_{\ell}^{\dagger} = \frac{1}{\sqrt{2}} (Q_{\ell} + iP_{\ell}), \quad (12)$$

where  $\Delta = (\Delta_x, \Delta_y)$  denotes a 2D position vector of the electron relative to the hole created at the  $\ell$ th site, and  $m$  is the number of phonons at the same site.  $|0\rangle$  denotes the electron-hole-phonon vacuum.  $k_p$  is the wave vector of photon which creates this excitation and  $k_p \rightarrow 0$  as mentioned before. Hence the electron-hole-phonon coupled state generated by a visible photon has full translational symmetry just same to that of the lattice. As seen from the above equation, we take only the charge-transfer excitation to the first layer from the second. We also assume that the phonon number  $m$  can become non-zero only when the electron and the hole are in the same site spanning two layers, that is,  $\Delta$  is zero. Since  $\Delta$  runs all over the 2D lattice sites, it can describe a largely distant free electron-hole pair, as well as an exciton heavily dressed in  $m(\gg 1)$  phonons.

Using this basis set, we calculate the matrix elements  $\langle \Delta, m | H | \Delta', m' \rangle$  of the Hamiltonian. By diagonalizing the matrix, we obtain a set of eigenvalues  $E_n$  and corresponding eigenstates  $|n\rangle$ . Then, we can calculate the time development of an electron-hole-phonon coupled state, which starts from the Franck-Condon state ( $\equiv |\Psi(0)\rangle$ ) at time  $t=0$ .

$$|\Psi(t)\rangle = e^{-iHt} |\Psi(0)\rangle = \sum_n e^{-iE_n t} |n\rangle \langle n | \Psi(0)\rangle. \quad (13)$$

Our main interest is to calculate the probability that the electron and the hole remain at the same site ( $\Delta=0$ ). The probability is defined as

$$\begin{aligned} n_{ex}(t) &\equiv \langle \Psi(t) | \sum_m |0, m\rangle \langle 0, m | \Psi(t) \rangle \\ &= \sum_{n, n', m} \langle \Psi(0) | n \rangle \langle n | 0, m \rangle \langle 0, m | n' \rangle \langle n' | \Psi(0) \rangle e^{-i(E_n - E_{n'})t}. \end{aligned} \quad (14)$$

This represents the probability of the self-localization of the electron-hole pair. We also define the average phonon number when the self-localization occurs as

$$\begin{aligned} n_{ph}(t) &\equiv \frac{1}{n_{ex}(t)} \langle \Psi(t) | \sum_m |0, m\rangle m \langle 0, m | \Psi(t) \rangle \\ &= \frac{1}{n_{ex}(t)} \sum_{n, n', m} \langle \Psi(0) | n \rangle \langle n | 0, m \rangle m \langle 0, m | n' \rangle \\ &\quad \times \langle n' | \Psi(0) \rangle e^{-i(E_n - E_{n'})t}. \end{aligned} \quad (15)$$

Practical calculations are performed by using  $80 \times 80$  sites with a periodic boundary condition for  $\Delta$ , and 200 phonon states.

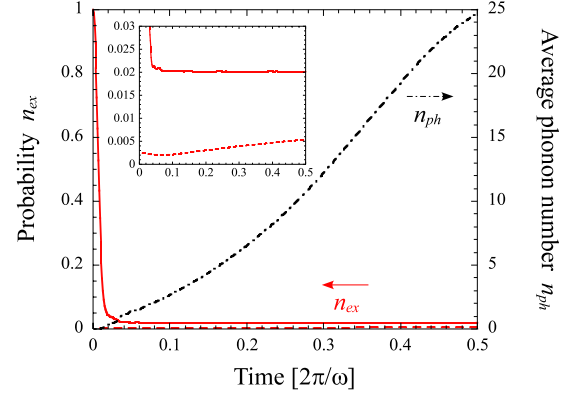


FIG. 2. (Color online) The probability  $n_{ex}$  that an electron and a hole remain at the same site spanning two layers (solid line) and the average phonon number  $n_{ph}$  (dashed-dotted line) as a function of time  $t [2\pi/\omega]$ . The dashed line, which is almost zero for this time interval, shows the result of the picosecond pulse excitation. The inset shows the closeup for  $n_{ex}$ .

## B. Results and discussions

First, as an initial state of the time development, we take an exciton wave packet  $|\Psi(0)\rangle = |\Delta=0, m=0\rangle$ , instantaneously created by a femtosecond photon pulse at time  $t=0$ . The energy of this initial state  $|0, 0\rangle$ , being not an eigenvalue of  $H$ , is given by

$$\bar{E}_{(0,0)} \equiv \langle 0, 0 | H | 0, 0 \rangle = \sum_n |\langle 0, 0 | n \rangle|^2 E_n, \quad (16)$$

with the mean-energy width,

$$\Delta \bar{E}_{(0,0)} \equiv \sqrt{\sum_n |\langle 0, 0 | n \rangle|^2 (E_n - \bar{E}_{(0,0)})^2}. \quad (17)$$

$\bar{E}_{(0,0)} \pm \Delta \bar{E}_{(0,0)}$  are estimated at about  $3.3 \pm 1.8$  eV, respectively. In the case of the femtosecond pulse, the energy width of the excitation light is  $O(1)$  eV. Thus, this initial state just corresponds to the femtosecond pulse excitation.

In Fig. 2, the probability  $n_{ex}$  and the average phonon number  $n_{ph}$  are plotted by solid and dashed-dotted lines, respectively, as a function of time  $t$ , where the unit of time is  $2\pi/\omega$  ( $\sim 42$  fs). In this calculation, the physically meaningful time region is from  $t=0$  to about a half period of  $2\pi/\omega$ , since there is no energy dissipation effect in our minimum model. In this time interval, we can see that the probability  $n_{ex}$  rapidly decreases from 1 to about 0.02 within a few femtoseconds, and the average phonon number  $n_{ph}$  rapidly increases simultaneously. This early-time decrease in  $n_{ex}$  is nothing but the free carrier relaxation process characteristic of the good conductor. This process is the most dominant, but  $n_{ex}$  does not reach zero and stabilizes at around 0.02. That is, the electron and the hole are bound with each other at the same site spanning two layers through the interlayer Coulomb attraction, creating a lot of phonons. This is nothing but the self-localization of the electron-hole pair. Hence, it is possible that the electron-hole pair excited in the 2D semimetallic continuum state causes the distortion that the two layers locally approach each other. Although we per-



formed our calculation in the 2D square lattice, the qualitative behavior does not change even in the 2D hexagonal lattice of the graphite.

Thus, our result shows that the relaxation of the electron-hole pair branches into the free carrier dissipation and the self-localization within a few femtoseconds. Once this branching occurs, these two channels are completely separated and can never be mixed up again because the self-localized electron-hole pair is heavily dressed in phonons. When the heavily dressed electron-hole pair tries to move to a neighboring site, it has to annihilate all these phonons and has to make them again at the neighboring site newly. This probability (quantum coherency) is almost zero. It is the spontaneous translational symmetry breaking, and finally makes a classical and local picture valid.

Next, we also consider the picosecond pulse excitation case, which is known to give no effect on the phase transition in the experiment.<sup>10</sup> In this case, the excitation includes the states with very large  $|\Delta|$ . Here, we make an initial state by using a Gaussian filter with the energy width  $\Delta E$  corresponding to the pulse width as

$$|\Psi(0)\rangle = \alpha \sum_{\Delta} |\Delta, 0\rangle \langle \Delta, 0| \sum_n e^{-((E_n - E_{ex})/\Delta E)^2} |n\rangle, \quad (18)$$

where  $E_{ex}$  is the excitation energy and  $\alpha$  is a normalization constant determined under  $\langle \Psi(0) | \Psi(0) \rangle = 1$ . In our calculation, we set  $E_{ex} = 3.3$  eV and the pulse width to 1 ps, leading to  $\Delta E$  of about  $10^{-3}$  eV. The time development of the probability  $n_{ex}$  in this case is also plotted by a dashed line in Fig. 2. As seen from this figure, the electron-hole pair is almost not excited at the same site and does not self-localize in this time interval. Therefore, it is also shown in our calculation that the picosecond pulse excitation gives no effect on the self-localization.

#### IV. INTERLAYER BOND FORMATION

Now, we have already seen the quantum logic of the self-localization. It is often misunderstood to be a sudden shrinkage of the excitation energy or the excitation wave function from the infinitely extended Bloch state to the localized state within a lattice site, for example, localized at the origin of the crystal. This picture of sudden shrinkage is, however, completely wrong and also against the general law of the special relativity that no motion can be faster than the light velocity. Before, during and even after the self-localization, the wave function never shrinks. Its square (the probability density of the excitation at each lattice site of the crystal) is always inversely proportional to  $N$  (volume) of the crystal, being normalized to be one within the whole crystal.

The difference between the extended Bloch state and the localized state occurs only in the presence or the absence of the intersite quantum phase coherence. The quantum phase coherence between the sites is 100% before the self-localization, while it becomes zero after the self-localization. In this stage, all the sites are quantum statistically independent and entirely equivalent. Thus, as the representative of all the sites, we can assume that the electron-hole pair is localized only at a site, that is, at the origin of the crystal, and can be treated classically.

What we finally obtain, after this self-localization, is the two carbons spanning two layers, largely displaced into the inside between the two layers. These two carbons have a large kinetic energy or a velocity toward the inside of the two layers. While, the electron and the hole are localized around these two carbons, for the reason that we have already explained in connection with the origin of the anharmonicity in Eq. (6). The electron and the hole are almost overlapped with each other, and hence, these two carbons are almost neutral.

In our previous two papers,<sup>15,16</sup> we have already shown that our system has no real energy gap, even if the two graphite layers have locally contracted to form the diaphite domain. Hence, the presence of localized exciton gives no serious effect in this final stage, as far as all the carbons keep almost neutral. It is quite in contrast to the starting Franck-Condon state, wherein the presence of exciton has given quite important effects.

In this stage, we can approximately replace the whole state by the classical motion of a graphite type carbon cluster, whose initial condition is the aforementioned inward displacement and velocity of the central two carbons. The original energy donated at the Franck-Condon excitation is now converted into the distortion and the velocity. Although the probability of the self-localization is fractional, the energy conservation law exactly holds even for this fractional component. However, because of the quantum uncertainty, these classical initial conditions should also reflect a large uncertainty around the given Frank-Condon energy  $\bar{E}_{(0,0)} \pm \Delta \bar{E}_{(0,0)}$ . Some part of them will be subsequently dissipated into surrounding carbons as ordinary phonons, but some part will surely remain as the stable interlayer  $\sigma$  bond.

In this section, by using a classical MD, we investigate how the interlayer bond is formed at around the self-localized site. Here, we also adopt the semiempirical Brenner's potential<sup>9</sup> in the MD.

##### A. Initial condition

We consider only two graphite layers with  $AB$  stacking and assume that due to the self-localization the interlayer distance contracts locally at the origin of the crystal. Then, as shown in Fig. 1(a), the two opposite carbons at the origin are intruded inside of the two layers and have a velocity toward the inside. As an initial condition, therefore, we give the two opposite carbons initial distortion (potential energy) and initial kinetic energy. Since we consider the simplest and ideal case in our calculation, we also assume that the initial displacements and initial velocities of the two carbons are in opposite direction, but have the same magnitude, that is, there is no phase shift in the initial condition. The initial kinetic energy  $K_0$  is given by  $K_0 = 2 \frac{1}{2} m_c v_0^2$ , where  $m_c$  is the mass of a carbon atom and  $v_0$  is the initial velocity. The initial potential energy is obtained from the relation between the intrusion and the potential energy calculated by using the Brenner's theory [dashed line in Fig. 1(b)]. As mentioned above, we assume that the energy of the electron-hole pair excited at a Franck-Condon state is converted into the lattice vibration through the self-localization process, so that we approximately regard the sum of the initial kinetic and the

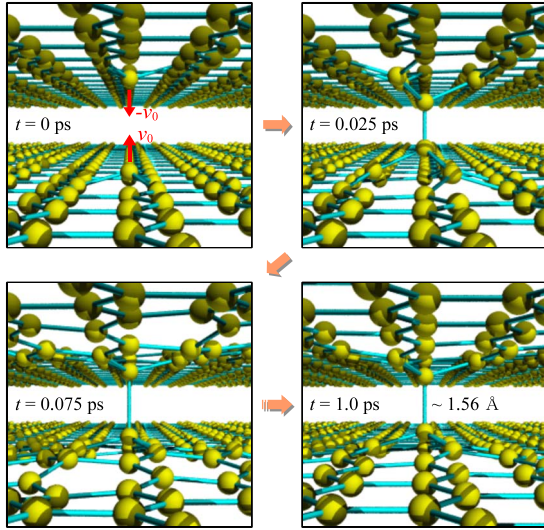


FIG. 3. (Color online) The snapshots of the MD calculation at time  $t=0, 0.025, 0.075,$  and  $1.0$  ps in the case of the initial kinetic energy of  $3.2$  eV and the initial intrusion of  $0.4$  Å. We display the bond between carbons when the intercarbon distance is within  $2$  Å.

potential energies as the excitation energy including the uncertainty. In our calculation, the total energy is conserved since we do not take into account any energy dissipation effects such as friction or a heat bath. The system consists of two graphite layers with the initial interlayer distance of  $3.35$  Å, and each layer includes  $2160$  carbons, wherein a periodic boundary condition is imposed.

**B. Results and discussions**

As an example that the interlayer bond is successfully formed, we show the result for the initial condition that the kinetic energy is  $3.2$  eV and the potential energy is  $1.54$  eV, corresponding to the initial intrusion of  $0.4$  Å as shown in Fig. 1(b). Figure 3 shows the snapshots of the MD calculation at time  $t=0, 0.025, 0.075,$  and  $1.0$  ps, where we can see that the interlayer bond is formed at  $t=1.0$  ps. In Fig. 4, we show the time development of the bond length between the two opposite carbons at the origin as a function of time on a logarithmic scale. The inset shows the same plot from  $0$  to  $0.1$  ps on a linear scale. The bond length decreases from  $2.55$  Å rapidly, and it settles down gradually in about  $1.56$  Å, repeating vibration. This bond length almost corresponds to that of the diamond structure ( $1.54$  Å). For comparison, we show the case of the initial kinetic energy of  $2.4$  eV, which does not result in the bond formation, by a dashed line in Fig. 4. In this case, the system does not overcome the energy barrier to form a bond due to the lack of energy and returns to the graphite without the bond formation.

Figure 5 shows the spread of the kinetic energy as a function of time. The solid line indicates the sum of the kinetic energies of the two opposite carbons at the origin, and the dotted line indicates that of the carbons located within a  $3a$  radius away from the origin except the two central carbons, where  $a$  is the lattice constant of the graphite ( $1.42$  Å). The one-dotted-dashed line and two-dotted-dashed line are those

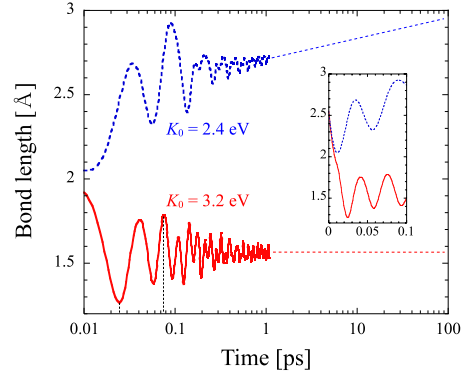


FIG. 4. (Color online) The bond length between the two opposite carbons at the origin as a function of time on a logarithmic scale. The inset shows the same plot from  $0$  to  $0.1$  ps on a linear scale. A solid line denotes the case of the initial kinetic energy of  $3.2$  eV and the initial intrusion of  $0.4$  Å and a dashed line is the case of the initial kinetic energy of  $2.4$  eV and the same intrusion. The two vertical dashed lines are corresponding to the time points of the snapshots at  $0.025$  and  $0.075$  ps in Fig. 3, respectively.

of carbons located in the radii between  $3a$  and  $6a$  and between  $6a$  and  $9a$ , respectively. The dashed line is that of carbons outside of a  $9a$  radius. The corresponding figure about these radii is shown in the inset of Fig. 5. Each curve is averaged in every  $0.02$  ps to eliminate fast vibrational behavior so that it is easy to see. As seen from this figure, the kinetic energy of the two central carbons decreases rapidly in the same time scale as the decrease in the bond length in the inset of Fig. 4, being spent on overtaking the barrier to form a bond. Simultaneously, the extra energy spreads to the near carbons through the intercarbon interaction derived from the Brenner’s potential, making the bond stable. Similarly, it moves to more outside carbons one after another. Thus, the kinetic energy which is initially given only to the two central carbons spreads all over the system as time passes. This

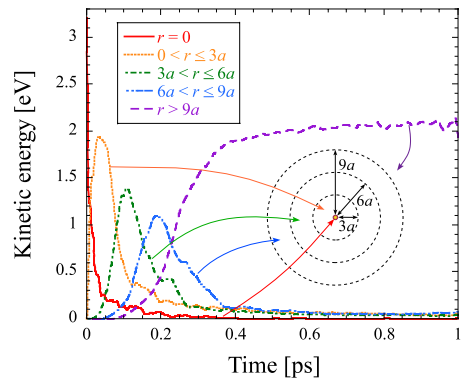


FIG. 5. (Color online) The kinetic energies as a function of time. The solid line indicates the sum of the kinetic energies of the two opposite carbons at the origin and the dotted line indicates that of the carbons located within a  $3a$  radius of the self-localized center except the two central carbons. The one-dotted-dashed line and two-dotted-dashed line are those of carbons located in the radii between  $3a$  and  $6a$  and between  $6a$  and  $9a$ , respectively. The dashed line is that of carbons outside of  $9a$  radius. The corresponding figure about these radii is shown in the inset.

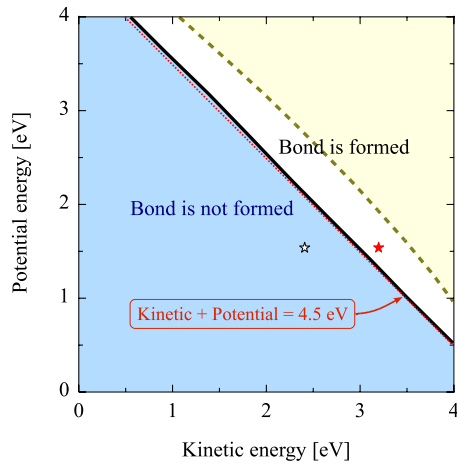


FIG. 6. (Color online) The relation between the initial energy and the interlayer bond formation. The horizontal and vertical axes indicate the initial kinetic and potential energies, respectively, given to the two central carbons. The filled and open stars denote the corresponding points of the two examples with and without the bond formation, respectively, mentioned in the text.

means that a great number of carbons around the self-localized point act as an energy reservoir to stabilize the bond formation. As seen from Fig. 5, the total energy dissipated into this reservoir is about 2 eV, while the energy used for the  $\sigma$ -bond formation is also about 2 eV, being consistent to the previous result.<sup>16</sup>

As mentioned before, the initial energy has some width because of the uncertainty for the excitation energy. Therefore, we performed the same calculations for various values of the initial kinetic and potential energies. Figure 6 shows the relation between the initial energy and the interlayer bond formation. The horizontal and vertical axes indicate the initial kinetic and potential energies, respectively, given to the two central carbons. The filled and open stars denote the corresponding points of the two examples with and without the bond formation, respectively, mentioned above. In the white region of this figure, sandwiched by thick solid and dashed lines, the interlayer bond can be formed successfully, while the other region denotes the condition that the bond is not formed. In the lower left part under the thick solid line, the total initial energy is not enough to form the interlayer bond. As a dotted line in Fig. 6 shows, the energy of more than about 4.5 eV can overcome the barrier to form the bond. This corresponds to the energy of about three visible photons with 1.57 eV.

From this energy limitation, the interlayer bond is not always formed even if the self-localization occurs. According to our results in Sec. III, the electron-hole pair excited in the energy region of  $3.3 \pm 1.8$  eV self-localizes at the probability of about 2%. Only the component with the energy of more than 4.5 eV among this self-localized states has the possibility to form the interlayer bond, and its ratio  $\sum_n |\langle 0,0|n\rangle|^2 \theta(E_n - 4.5)$  is estimated to be about 26%, where  $\theta(x)$  is a unit step function. In this case, therefore, it is expected that 0.52% of the excitation contributes to the bond formation. Thus, we conclude that, at a small but finite probability, the interlayer bond can be formed.

In the upper right part above the thick dashed line in Fig. 6, the initial energy is so large that the bond is not formed due to the strong repulsion between the two carbons although the bond length once shrinks less than 2 Å.

## V. SUMMARY

We have theoretically clarified the early-stage dynamics of the interlayer  $sp^3$ -bond formation of graphite. We have studied the spontaneous translational symmetry breaking and the self-localization of the electron-hole pair excitation full quantum mechanically. The electron-hole pair excited by visible light at the Franck-Condon state dissipates into the semi-metallic continuum electronic states as free carriers. However, by a small probability of about 2%, it self-localizes by contracting the interlayer distance due to the Coulomb attraction. Moreover, we have found that the picosecond pulse excitation gives no effect on the self-localization.

We have calculated the subsequent interlayer bond formation by using the classical molecular dynamics with the semiempirical Brenner's potential. The interlayer  $\sigma$  bond can be formed when the appropriate excitation energy is given, and the energy is more than 4.5 eV corresponding to about three visible photons.

Thus, the tiny domain of the interlayer  $\sigma$  bond is locally photogenerated in the graphite layers by a few visible photons. Through further pulse excitation, this tiny domain may proliferate stepwise up to a new phase, namely, diaphite.

## ACKNOWLEDGMENTS

The authors thank K. Tanimura, J. Kanasaki, E. Inami, and H. Ohnishi for presenting their results prior to publication and valuable discussions. This work is supported by the Ministry of Education, Culture, Sports, Science and Technology of Japan, the peta-computing project, and Grant-in-Aid for Scientific Research (S), Contract No. 19001002, 2007.

<sup>1</sup>F. Bundy, J. Chem. Phys. **38**, 631 (1963).

<sup>2</sup>T. Irifune, A. Kurio, S. Sakamoto, T. Inoue, and H. Sumiya, Nature (London) **421**, 599 (2003).

<sup>3</sup>F. Banhart, J. Appl. Phys. **81**, 3440 (1997).

<sup>4</sup>H. Nakayama and H. Katayama-Yoshida, J. Phys.: Condens. Matter **15**, R1077 (2003).

<sup>5</sup>S. Fahy, S. G. Louie, and M. L. Cohen, Phys. Rev. B **34**, 1191 (1986).

<sup>6</sup>S. Fahy, S. G. Louie, and M. L. Cohen, Phys. Rev. B **35**, 7623 (1987).

<sup>7</sup>Y. Tateyama, T. Ogitsu, K. Kusakabe, and S. Tsuneyuki, Phys. Rev. B **54**, 14994 (1996).

- <sup>8</sup>C. J. Mundy, A. Curioni, N. Goldman, I.-F. W. Kuo, E. J. Reed, L. E. Fried, and M. Ianuzzi, *J. Chem. Phys.* **128**, 184701 (2008).
- <sup>9</sup>D. W. Brenner, *Phys. Rev. B* **42**, 9458 (1990).
- <sup>10</sup>J. Kanasaki, E. Inami, K. Tanimura, H. Ohnishi, and K. Nasu, *Phys. Rev. Lett.* **102**, 087402 (2009).
- <sup>11</sup>L. Radosinski, K. Nasu, J. Kanazaki, K. Tanimura, A. Radosz, and T. Luty, in *Molecular Electronic and Related Materials-Control and Probe with Light*, edited by T. Naito (Transworld Research Network, India, 2009), Chap. 14.
- <sup>12</sup>K. Nasu, *Photoinduced Phase Transitions* (World Scientific, Singapore, 2004).
- <sup>13</sup>K. Nasu, *Rep. Prog. Phys.* **67**, 1607 (2004).
- <sup>14</sup>See Research highlight, *Nature* (London) **458**, 129 (2009).
- <sup>15</sup>H. Ohnishi and K. Nasu, *Phys. Rev. B* **79**, 054111 (2009).
- <sup>16</sup>H. Ohnishi and K. Nasu, *Phys. Rev. B* **80**, 014112 (2009).
- <sup>17</sup>N. Mataga and K. Nishimoto, *Z. Phys. Chem., Neue Folge* **13**, 140 (1957).
- <sup>18</sup>K. Cho and Y. Toyozawa, *J. Phys. Soc. Jpn.* **30**, 1555 (1971).